Numerical analysis on thermal and hydraulic performance of diverging-converging minichannel heat sink using Al_2O_3-H_2O nanofluid

Numerical analysis on thermal and hydraulic performance of diverging-converging minichannel heat sink using Al_2O_3-H_2O nanofluid

N M Muhammad[1, 2]* and N A C Sidik[1]

[1] Faculty of Engineering, Universiti Teknologi Malaysia, 81310 Skudai, Johor, Malaysia.
[2] Department of Mechanical Engineering, Kano University of Science and Technology, Wudil. PMB 3244. Nigeria.

*Corresponding author: nuramuaz@gmail.com

Abstract. Miniaturization as a size reduction of electronic devices components lead to high performance, but with increase in heat flux density which reduce the efficiency of these devices. Minichannel has been considered to improve the heat dissipation with minimal pressure drop through regulation of the channel configurations. In this study, a divergent-convergent minichannel heat sink (DCMCHS) was investigated numerically using Finite volume method to model single-phase forced convection for nanofluid cooling as a passive means to enhance the heat transfer performance for Reynolds number range of 2000 to 2300 and using Aqueous Alumina as nanofluid with concentrations of 0.1 – 0.8%. The effect of Reynolds number, the convection coefficient and pressure drop in relation to the heat flux were investigated and discussed. The results show that, Nusselt number increases with increase in volume fraction and Reynolds number, whereas friction factor decreased with increasing Reynolds number. Heat removal by the nanofluid is higher near the walls than in the central part of the minichannel, and the performance factor is between 1.00 – 1.01 and it increases with increase in concentration and flow velocity. Thus, combine passive techniques of DCMCHS and nanofluid provides better enhancement of heat transfer and hydraulic attributes of the minichannel heat sink for cooling purposes.

1. Introduction

Despite rapid technological advancements which creates better and efficient tools to enhance the condition of living of human, it is sometimes restricted with the limit of demand of rapid heat removal from such inventions. Conventional fluids or base fluids such as water and ethylene glycol failed to provide adequate removal of heat from electronic devices and heat exchangers. Nanofluid is an innovative engineering thermal fluid formed by dispersing nanosized materials, usually 1-100 nm in conductive base fluid; and has exhibited remarkable attributes in efficient removal of heat from thermal systems.

Removal of heat or enhancement from thermal systems can be achieved through either active or passive techniques. The former requires external systems like pumps, while the latter which is more of variation of geometry and surface treatments, hence its more applied due to energy serving. It was observed by Keblinski et al. [1] that factors that increases thermal conductivity of nanofluid include: Brownian motion, clustering of nanoparticles, nature of heat transport in the nanoparticles and formation

of molecular-level layer of the liquid at the liquid-particles interface. To further enhance heat transfer through passive techniques, researchers combine use of nanofluids with multi configuration channels such as micro and mini channels [2-4].

Alumina (Al_2O_3) is one of the commonly used nanoparticle because of its high reactivity and thermal conductivity amongst other metallic oxide nano particles. Sohel et al. [5] reported enhancement of heat transfer coefficient by 18% at 0.25% volume fraction of Al_2O_3-water, while Vafaie et al. [6] indicated 40% heat transfer enhancement in fully developed regime of the laminar flow. Other researchers used the alumina and reported remarkable heat and flow enhancement. [7-9]. Dominic et al. [10] investigated the forced convective fluid flow on the heat transfer and flow pressure drop of divergent minichannels using nanofluids and reported that Nusselt number attained 76% maximum in laminar region when Al_2O_3-H_2O is used and 40% in turbulent region in divergent straight minichannel. Singhal and Ansari [11] investigated flow and pressure drop characteristics to determined characteristic length scale of non-uniform tapered microchannel by considering three cases of diverging, converging and equal sections of the pair under single generalized model. They used water as transport fluid at low flow rate and found that DCMCHS has least pressure drop compared to other cases. Ho et al. [12] conducted a comparative study on hydrothermal performance of a parallel and divergent minichannel heat sinks (MCHSs) with divergence angle (β) from 0° (parallel) to 1.38° and 2.06°. They concluded that the divergent MCHSs are better than the conventional parallel MCHSs for practical thermal applications by offering greater values of Nusselt number and COP with lower pressure drop penalty, especially at higher Reynolds number of the working fluid.

In a another work [13], they extended the influence of diverging minichannels on the contribution of microencapsulated phase change material (MEPCM) suspensions in heat sinks using same divergence angle and found that the suppression of wall temperature profile increased by up to 33% in the diverging cross-section of channels. Ermagan and Rafee [14] studied the thermal efficiency of converging microchannels with superhydrophobic walls under various coolant flow rates and found that the thermal performance enhancement was attained only for a low pumping power (Ω<0.5 Watts). Also, Dehgan et al. [15] employed Alumina and converging passage microchannel as combine passive technique to enhance conjugate heat transfer and they revealed that an effective enhancement on the convection heat transfer coefficient as high as 2.35 fold than that of a pure water in a straight channel. Some researchers tried to combine the diverging and converging passage in their researches on hydrothermal performance with varying conditions and revealed remarkable results. The Study of heat transfer enhancement in periodic converging-diverging microchannel was conducted by Chandra et al. [16] and they reported that average Nusselt number doubles in one of the channels than the classical value, and there is stronger recirculation and separation of flow due to influence of converging-diverging cross-section. Chai et al. [17] carried out a 3-D numerical study on the heat transfer characteristics of laminar flow in microchannel heat sinks using different geometric fan-shaped (similar to convergent and divergent shape) ribs on sidewalls for Reynolds number within 187 to 715. They reported that, average Nusselt number increased by 6–101% and total thermal resistance decreased by 3–40%. The advantage of the thermal conductivity of the alumina motivate us to employ it in the research of diverging-converging minichannel heatsink for cooling purposes.

From the above, all the researches that used diverging-converging passages are done in microchannel scale with none in minichannel scale, hence, to the best of authors' knowledge from the available literatures, no research was conducted using the proposed geometry and Alumina as combine passive heat transfer enhancement techniques within the fully developed laminar region. In this paper, the modelling of 3D single-phase laminar flow containing metallic-oxide nanofluid with three different volume fractions and variation of Reynolds number for $2000 \leq Re \leq 2300$ was numerically investigated using commercial CFD tool (ANSYS-FLUENT v17.1) in a diverging-converging minichannel, with the objective of studying the effect of nanofluid concentration on heat transfer and hydraulic flow.

2. Mathematical modelling

2.1 Model geometry

The schematic designs of the divergent-convergent minichannel heat sinks (DCMCHS) having dimensions of $L\times W\times H_b$=30mm×30 mm×2.25 mm having 10 parallel channels each of width and height of 1mm and 1.25mm, respectively as illustrated in Figure 1. The DCMCHS includes uniformly heated base and adiabatic cover plates. The nanofluid passes through the channels of heat sink made of up aluminium and remove heat by convection from a heat dissipating component (chip) that is attached to the bottom of the heat sink. Since the minichannels are made-up to be identical in terms of both heat transfer and hydrodynamics, thus, only one of the channels is used as computational domain as shown in Figure 1(b).

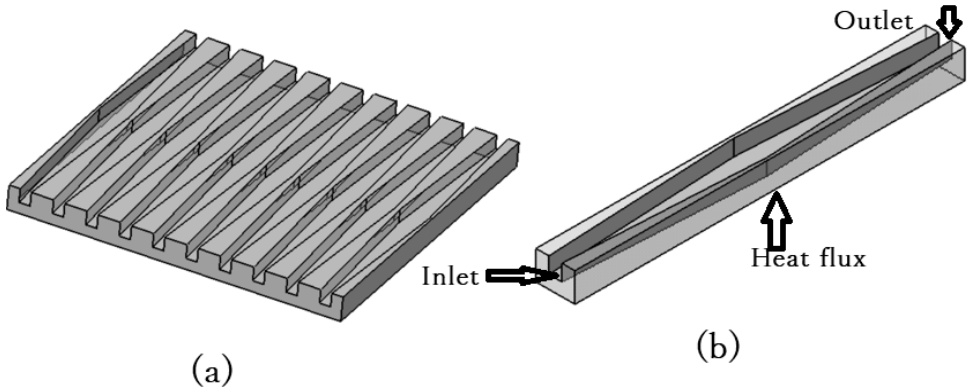

Figure 1 (a) 3D Schematic design of diverging-converging minichannel heat sink and (b) Computational domain.

The geometry is characterised with certain restrictions such as, equal angle of divergence and convergence (6°), length of 30 mm, while hydraulic diameter is determined from the trapezoidal section at the midplane of either the divergent or convergent section [18]. Thus:
Area:

$$A = \frac{1}{2} * (W_t + W_b) * \dot{H} \tag{1}$$

Wetted Perimeter:

$$P = (W_t + W_b) + 2 * \dot{H} \tag{2}$$

And, the hydraulic diameter can be obtained as:

$$D_h = \frac{4\mathrm{A}}{\mathrm{P}} = \frac{2(\acute{W}\cdot\dot{H})}{\acute{W}\cdot\dot{H}} \tag{3}$$

where: $\dot{H}$, W_t and W_b represent the slant height, widths at top and bottom sections of the fluid domain. Table 1 illustrated the geometrical values used in the study.

Table 1. Geometrical details of the configuration

Geometry	W_t (mm)	W_b (mm)	α	θ (°)	W(mm)	$\dot{H}$(mm)	D_h(mm)
Divergent-Convergent	1.79	1.78	0.50	6	3.57	1.24	1.46

2.2 Governing equations

The steady state conservation equations for mass, momentum and energy in fluid are respectively presented as follows:

Continuity equation given by:

$$\frac{\partial u}{\partial x}+\frac{\partial u}{\partial y}+\frac{\partial u}{\partial z}=0 \tag{4}$$

whereas momentum equations in x, y and z components, respectively are given as:

$$u\frac{\partial u}{\partial x}+v\frac{\partial u}{\partial y}+w\frac{\partial u}{\partial z}=-\frac{1}{\rho}\frac{\partial p}{\partial x}+\frac{\mu}{\rho}\left(\frac{\partial^2 u}{\partial x^2}+\frac{\partial^2 u}{\partial y^2}+\frac{\partial^2 u}{\partial z^2}\right) \tag{5a}$$

$$u\frac{\partial u}{\partial x}+v\frac{\partial u}{\partial y}+w\frac{\partial u}{\partial z}=-\frac{1}{\rho}\frac{\partial p}{\partial y}+\frac{\mu}{\rho}\left(\frac{\partial^2 v}{\partial x^2}+\frac{\partial^2 v}{\partial y^2}+\frac{\partial^2 v}{\partial z^2}\right) \tag{5b}$$

$$u\frac{\partial u}{\partial x}+v\frac{\partial u}{\partial y}+w\frac{\partial u}{\partial z}=-\frac{1}{\rho}\frac{\partial p}{\partial z}+\frac{\mu}{\rho}\left(\frac{\partial^2 w}{\partial x^2}+\frac{\partial^2 w}{\partial y^2}+\frac{\partial^2 w}{\partial z^2}\right) \tag{5c}$$

where u, v and w are the velocity components in x, y and z directions, respectively. In addition, the pressure drop, weight density and dynamic viscosity of the fluid are represented with p, ρ and μ, respectively.

Energy equation for the fluid:

$$u\frac{\partial T}{\partial x}+v\frac{\partial T}{\partial y}+w\frac{\partial T}{\partial z}=\frac{k_f}{\rho Cp}+\left(\frac{\partial^2 T}{\partial x^2}+\frac{\partial^2 T}{\partial y^2}+\frac{\partial^2 T}{\partial z^2}\right) \tag{6}$$

Energy equation for the solid:

$$k_s\left(\frac{\partial^2 T}{\partial x^2}+\frac{\partial^2 T}{\partial y^2}+\frac{\partial^2 T}{\partial z^2}\right)=0 \tag{7}$$

where T, k_f and k_s are temperature, and thermal conductivities of fluid and solid materials, respectively.

2.3 Boundary conditions

Three boundary conditions are applied to close the above mathematical equations. At the inlet boundary, temperature and pressure of the nanofluid are specified as 30°C (303K) and 1 bar respectively, while "Pressure outlet" is imposed at the outlet with 0 Pa (gauge pressure). A constant heat flux of 45 kW/m^2 is applied on the bottom wall while, for all other walls, no slip condition (viscous flow) is experienced, thus velocity gradient forms in fluid and exerts flow resistance as pressure drop. All variables are initiated from the inlet boundary condition.

2.4 Thermophysical properties of fluid

The working fluid used in this simulation is aqueous alumina (Al_2O_3-H_2O) nanofluid with volume fractions of 0.001, 0.005 and 0.008. It is assumed that the nanofluid is in thermal equilibrium with zero relative velocity. The properties of nanofluid and the base fluid (water) considered in the present study are the ones used by Abdelrazek et al. [19] and presented in Table 2.

Table 2. Thermophysical properties of water and nanoparticle at Temperature of 27°C [19]

Materials	Density (kg/m^3)	Specific heat (J/kgK)	Thermal conductivity (W/mK)	Viscosity (kg/ms)	Particle size (nm)
Water (H_2O)	995.8	4178.4	0.615	8.03E-04	-
Alumina (Al_2O_3)	3970	765	36	-	<50

The thermo-physical properties of nanofluid are calculated using the relations below:
The density of Al_2O_3/water nanofluids Equation (8) was determined using model developed by Pak et al. [20]:

$$\rho = (1-\phi)\rho_{bf} + \phi\rho_p \quad (8)$$

The specific heat of the nanofluids Equation (9) was calculated using Xuan and Roetzel. [21]:

$$Cp_{nf} = \frac{\phi(\rho Cp)_p + (1-\phi)(\rho Cp)_{bf}}{\rho_{nf}} \quad (9)$$

The thermal conductivity of the nanofluid (k_{nf}) was calculated using the Maxwell model [22] for nanofluids with volume fraction less than unity and considering Brownian motion where n=3 for spherical Al_2O_3, and is given by Equation (10) as follows:

$$k_{nf} = \frac{k_p + (n-1)k_{bf} - \phi(n-1)(k_{bf}-k_p)}{k_p + (n-1)k_{bf} + \phi(k_{bf}-k_p)} k_{bf} \quad (10)$$

The viscosity of the nanofluids, Equation (11) was calculated using the viscosity correlation proposed by Maiga et al. [23] as follows:

$$\mu_{nf} = \mu_w(1 + 7.3\phi + 123\phi^2) \quad (11)$$

where, ϕ, Cp, k and ρ are the concentration of the nanoparticle, heat capacity, thermal conductivity, viscosity and density respectively. While subscripts bf, p and nf denotes the base fluid, the nanoparticle and nanofluid respectively.

3. Numerical approach

The three-dimensional forced convection flow and heat transfer were modelled using commercial CFD solver, ANSYS FLUENT 17 with the assumptions that: the working fluid is considered three-dimensional, incompressible, and Newtonian. It is flowing in steady state laminar condition. The thermophysical properties of heat sink and fluid are constant, while the effect of radiation heat transfer for fluid flow and the influence of gravity and other body forces are neglected. The finite volume method approach was employed in the simulation, where velocity and pressure fields where coupled using SIMPLE algorithm. A second-order upwind interpolation scheme is used for discretization of the convective and diffusive terms. The convergence criteria were set when the normalised residual values are below 10^{-6} for all the variables.

3.1 Grid independency

A hexahedral mapped mesh was used for all the simulations. Various grids of sizes from 600,000 to 1.228 million elements were used in checking the mesh independency of the solution to ensure that, the results obtained does not rely on the size and the number of generated cells. The variation in the Nusselt numbers between the solutions on the grids with 0.90 million and 1.2 million elements is found to be below 0.5% as shown in Table 3, hence, to save computing time and memory, grid sizes of around 0.90 million elements were used for all the simulations in this study. The meshing of the computational fluid domain employed in the analysis is shown in Figure 2.

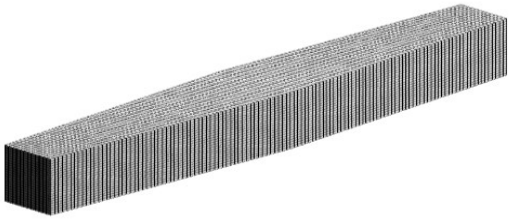

Figure 2. 3D Mesh of the fluid domain.

Table 3. Grid independency analysis

Mesh (**x**x**y**x**z**)	Pressure drop ΔP	ΔP error (%)	Surface Nusselt Number	Nu error (%)
M1 (64x64x300)	562.29	Baseline	11.82	Baseline
M2 (60x60x300)	559.86	0.43	11.84	0.11
M3 (60x50x300)	**559.86**	**0.43**	**11.84**	**0.11**
M4 (50x50x300)	559.86	0.43	11.84	0.11
M5 (50x40x300)	546.55	2.80	11.86	0.30

3.2 Validation

The precision and validity of the numerical results were validated through comparison with existing correlations in the literature due to non-availability of experimental results in diverging-converging minichannels. Sieder and Tate, and Hausen correlations [24] for fully developed laminar region were employed for Nusselt number enhancement, while Blasius relation [25] were used for frictional resistance; to substantiate the ability of the solver to accurately and reliably predict the results. The comparisons were performed with the friction factor and average Nusselt number for the range of Reynolds numbers in all the values of nanofluid concentrations and base fluid, as presented in Figure 3.

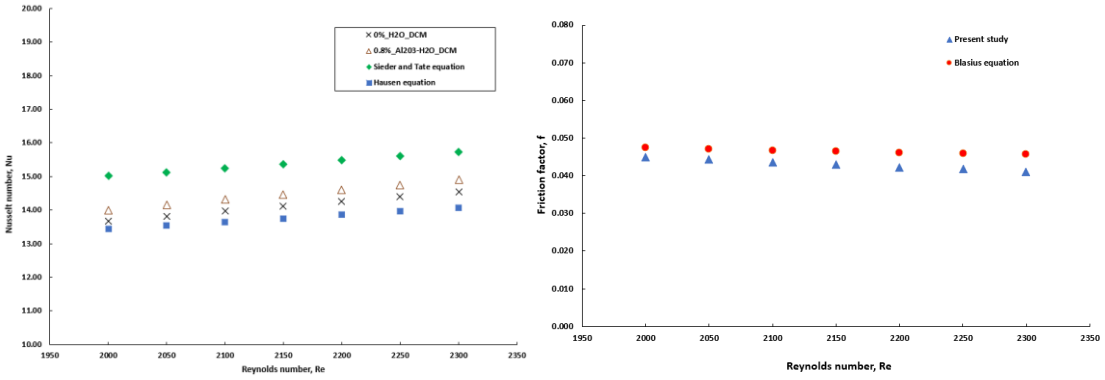

(a) (b)

Figure 3. Validation of results of (a) Nusselt number and (b) friction factor as functions of Reynolds number.

It can be observed from Figure 3 (a) that, Sieder and Tate correlation over predict the average Nusselt number at Re 2300 by about 5.2% for 0.8% concentration of the nanofluid and 7.4% higher for the base fluid. However, Hausen correlation under predict the average Nusselt number at the same Reynolds number by 6% and 3.5% for 0.8% concentration of the nanofluid and base fluid, respectively. Since the deviations of the average Nusselt numbers from the two correlations used is within ±10%, it can be considered that, the numerical results were appreciably well predicted by the method employed. For the friction factor, Figure 3 (b) indicates that, the numerical friction factor of the DCMCHS in the fluid shows appreciable agreement with the correlated results of Blasius, however, the deviation of the numerical friction factor from the theoretical values of nanofluid is around 5% and 10% lower at 2000 and 2300 Reynolds numbers, respectively. Perhaps, this could be due to the increase of pressure drops as the flow velocity increases at the entrance of the channel, and to the assumptions made in mathematical formulation of the simulation.

3.3 Data processing

The following Equations (12-17) were used to estimate the different important thermal and flow parameters of the minichannel heat sink.

The average heat transfer coefficient (h) and Nusselt number (Nu) were respectively obtained by:

$$\mathbf{h} = \frac{\mathbf{q}}{(\mathbf{T_w} - \mathbf{T_b})} \tag{12}$$

$$\mathbf{Nu} = \frac{\mathbf{hD_h}}{\mathbf{k}} \tag{13}$$

The base fluid velocity is estimated by using the relation of Reynolds number as follows:

$$\mathbf{Re} = \frac{\boldsymbol{\rho}\mathbf{uD_h}}{\boldsymbol{\mu}} \tag{14}$$

However, to take the influence of base fluid in the nanofluid formed, the nanofluid velocity is determined using the following expression:

$$\mathbf{u_{nf}} = \frac{\boldsymbol{\rho_{bf}}}{\boldsymbol{\rho_{nf}}} \frac{\boldsymbol{\mu_{nf}}}{\boldsymbol{\mu_{bf}}} \mathbf{u_{bf}} \tag{15}$$

While, pressure drop was determined from Darcy-Weisbach relation which relates the drops in pressure to frictional resistance in the flow as:

$$\Delta\mathbf{P} = \frac{\mathbf{f}\boldsymbol{\rho}\mathbf{u^2}}{\mathbf{2}} \left(\frac{\mathbf{L}}{\mathbf{D_h}}\right) \tag{16}$$

The performance of flow in the minichannel is evaluated using pumping power which can be determine as function of the differential pressure drop, frictional resistance and velocity of the flow. It's given as:

$$\mathbf{PP} = \Delta\mathbf{P} \cdot \mathbf{f} \cdot \mathbf{u} \tag{17}$$

where q, D_h, L, u, k, T_w and T_b are the heat flux, hydraulic diameter, channel length, fluid velocity, thermal conductivity of the fluid, average temperatures on the wall and bulk fluid respectively. Darcy friction factor (f) can be obtained from equation (16).

4. Results and discussion

The results were obtained using a single-phase method for concentrations of ϕ= 0.1, 0.5 and 0.8 % volume with the range of Reynolds numbers of 2000 – 2300 and heat flux of 45 kW/m^2.

4.1 Effect of nanofluid concentration

The concentration of the nanofluid shows a linear relationship with the Nusselt number and Heat transfer coefficient as shown in Figure 4 (a) and (b), respectively. As volume concentration and flow velocity increases, the surface heat transfer coefficient (HTC) also increases, with highest increment of about 3% at Re of 2300 and concentration of 0.8 %. Similarly, the Nusselt number also enhances with increase in nanofluid concentration due to increase in fluid velocity and mixing of flow, though the enhancement in terms of Nusselt number is small due to the dominance of thermal conductivity of nanofluid over the base fluid. However, the data at Re 2000 and 0.5% nanofluid shows little bit different trend and this could be due to the variation of velocity which increases by merely 0.5% from 0% concentration to about 2% up to 0.5% concentration, and appreciably raised to 4% at 0.8% concentration.

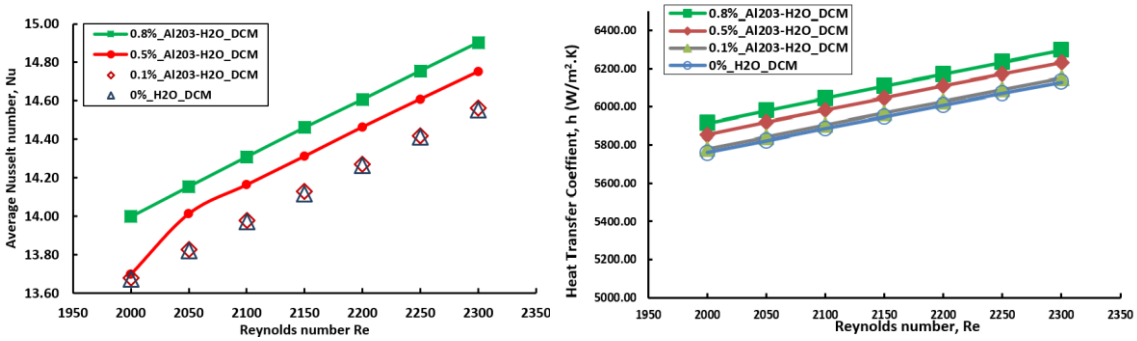

Figure 4. Effect of nanofluid concentrations on (a) average Nusselt number and (b) Heat transfer coefficient.

4.2 Pressure drops

The variation of pressure drops as a function of Reynolds number is illustrated in Figure 5. Its obtained as the difference between the inlet and outlet channel pressures. Though, the total pressure drop involves aggregated effects of entrance and exit losses, effects at the developing region and frictional losses as depicted in Equation (15). Increase in physical properties of nanofluid over water particularly viscosity and density, also leads to the increase in pressure drop from about 1% to about 7 % for the concentrations of 0.1 % and 0.5 %, respectively. There is highest increase of about 11% in pressure drop as the velocity increases in 0.8% concentration. This is due to expansion and contraction of the flow passage which though disturb the boundary layer and enhances the heat transfer, but the small hydraulic diameter is responsible for the drops in pressure. However, from the Equation (15), the relationship between the pressure drop and friction factor is directly proportional, but this works indicated contrary, because the geometry used has converse relation to that due to increment in surface area coupled with the decrease in flow velocity.

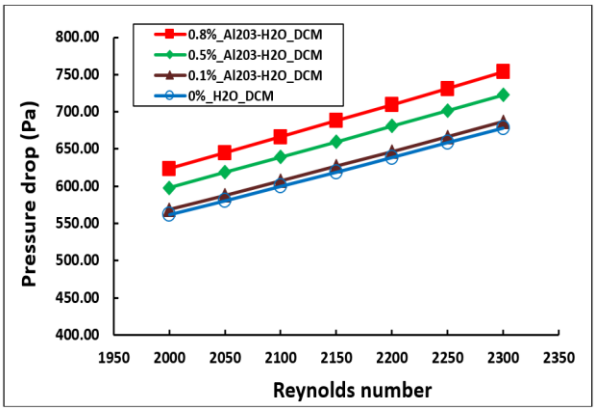

Figure 5. Variation of Pressure drop with Reynolds number.

Reynolds number as the ratio of inertial to viscous forces is used to determine the flow velocity, and due to the lower velocities, mostly below 1.5 m/s, the viscous forces predominates, hence less pressure force occurred within the minichannel causes minimal drop in pressure. From Figure 6, it can be observed that, both the velocity and pressure profiles indicate non-linear changes from the inlet to the outlet of the DCMCHS. Deceleration and acceleration (due to divergence and convergence, respectively) of the flow at the middle of the minichannel causes recirculation and vortices creation which enhances flow mixing but leads to high pressure. However, the velocity is higher at the exit due

to the convergence effect of the passage which causes acceleration of the flow but highlighted a developing flow throughout the flow channel as shown in Figure 6 (b).

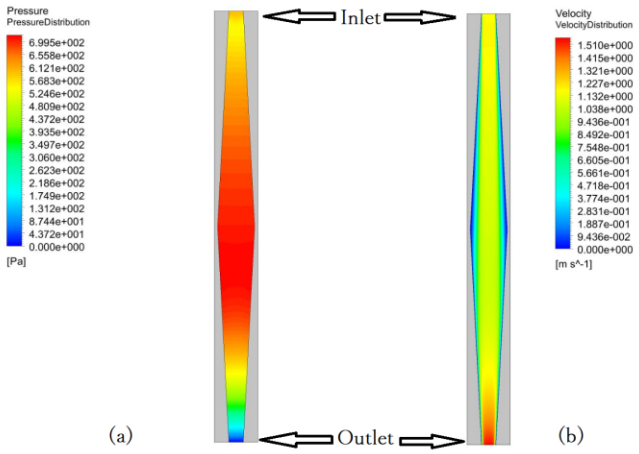

Figure 6. Contours of (a) Pressure and (b) Velocity at Re 2300 and 0.8%.

4.3 Performance factor

The thermal enhancement represented by Nusselt number *Nu* and friction factor *f* are employed to assess the performance of flow of fluids and heat transfer.[26], its expressed as:

$$\eta = \frac{(Nusselt\ no)_{nf}/(Nusselt\ no)_{bf}}{\left((Friction\ resistance)_{nf}/(Friction\ resistance)_{bf}\right)^{1/3}} \tag{17}$$

where, subscripts nf and bf represent nanofluid and base fluid, respectively.

As indicated in Figure 7, it was found that the performance factor is between 1.00 – 1.01 and it increases with increase in concentration and flow velocity. Since, the performance factor is above unity, it indicates the applicability of the geometry in enhancement of heat transfer.

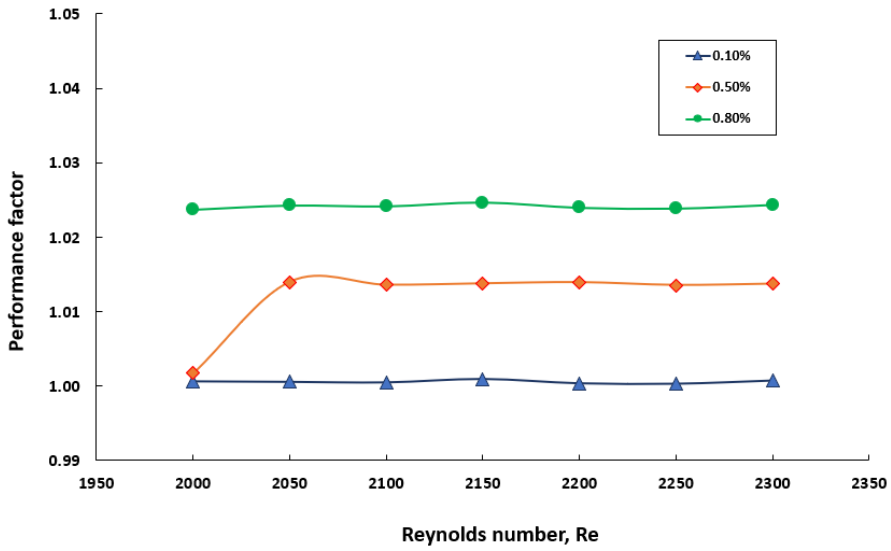

Figure 7. Performance factor.

5. Conclusions

Numerical analysis of heat transfers and fluid flow characteristics of divergent-convergent minichannel heat sink (DCMCHS) has been studied using aqueous Alumina as nanofluid, and the following conclusions were made:

- There is a significant influence of Reynolds number on heat transfer enhancement on both the base fluid and the nanofluid. Deceleration and acceleration of the flow at the middle of the channel causes recirculation and vortices creation which enhances flow mixing.
- There is slight increase in friction factor which may be linked to non-uniformity of channel passage due to divergence and convergence nature, and it decreases with increase in Reynolds number. The trend is similar across all the volume fractions.
- The enhancement in heat transfer coefficient of about 3% is due to influence of nanofluid in DCMCHS and increase in thermal conductivity of the nanofluid over water.
- The Performance factor which is a factor to indicate the augmentation in heat transfer of nanofluid over base fluid was found to be 1.01
- Better enhancement in heat transfer and hydrodynamic influence could be achieving and well predicted if the numerical analysis could be extended to turbulent regime and moderately higher volume concentration, say up to 5 %.

Acknowledgement:
The authors would like to express their appreciation for the support of the sponsors Malaysia-Japan International Institute of Technology, UTM with Project No: R. K130000.7343.4B314.

References

[1] Keblinski P, Phillpot S R, Choi S U S and Eastman J A 2002 Mechanisms of heat flow in suspensions of nano-sized particles (nanofluids) *International Journal of Heat and Mass Transfer* **45** 855-63.
[2] Ahmadi A A K, E. Moghadasi, H. Malekian, N. Akbari, O. A. and Bahiraei, M. 2018 Numerical study of flow and heat transfer of water-Al2O3 nanofluid inside a channel with an inner cylinder using Eulerian–Lagrangian approach *Journal of Thermal Analysis and Calorimetry* **132** 651-65.
[3] Khoshvaght-Aliabadi M, Rad S H and Hormozi F 2016 Al2O3–water nanofluid inside wavy mini-channel with different cross-sections *J Taiwan Inst Chem E* **58** 8-18.
[4] Ghaziani N O and Hassanipour F 2017 Convective Heat Transfer of Al2O3 Nanofluids in Porous Media *Journal of Heat Transfer* **139**.
[5] Sohel M R, Khaleduzzaman S S, Saidur R, Hepbasli A, Sabri M F M and Mahbubul I M 2014 An experimental investigation of heat transfer enhancement of a minichannel heat sink using Al2O3-H2O nanofluid *International Journal of Heat and Mass Transfer* **74** 164-72.
[6] Vafaei S and Wen D 2012 Convective heat transfer of aqueous alumina nanosuspensions in a horizontal mini-channel *Heat and Mass Transfer/Waerme- und Stoffuebertragung* **48** 349-57.
[7] Bahiraei M and Heshmatian S 2017 Optimizing energy efficiency of a specific liquid block operated with nanofluids for utilization in electronics cooling: A decision-making based approach *Energ Convers Manage* **154** 180-90.
[8] Ghasemi S E, Ranjbar A A and Hosseini M J 2017 Thermal and hydrodynamic characteristics of water-based suspensions of Al2O3 nanoparticles in a novel minichannel heat sink *Journal of Molecular Liquids* **230** 550-6.
[9] Khoshvaght-Aliabadi M, Hassani S M and Mazloumi S H 2017 Performance enhancement of straight and wavy miniature heat sinks using pin-fin interruptions and nanofluids *Chemical Engineering and Processing: Process Intensification* **122** 90-108.
[10] Dominic A, Sarangan J, Suresh S and Devah Dhanush V S. An experimental study of forced convective fluid flow in divergent minichannels using nanofluids. 2014. p. 1418-22.

[11] Singhal R and Ansari M Z 2016 Flow and Pressure Drop Characteristics of Equal Section Divergent-Convergent Microchannels *Procedia Technology* **23** 447-53.
[12] Ho C J, Chang P C, Yan W M and Amani P 2018 Thermal and hydrodynamic characteristics of divergent rectangular minichannel heat sinks *International Journal of Heat and Mass Transfer* **122** 264-74.
[13] Ho C J, Chang P C, Yan W M and Amani P 2018 Efficacy of divergent minichannels on cooling performance of heat sinks with water-based MEPCM suspensions *International Journal of Thermal Sciences* **130** 333-46.
[14] Ermagan H and Rafee R 2018 Effect of pumping power on the thermal design of converging microchannels with superhydrophobic walls *International Journal of Thermal Sciences* **132** 104-16.
[15] Dehghan M, Daneshipour M and Valipour M S 2018 Nanofluids and converging flow passages: A synergetic conjugate-heat-transfer enhancement of micro heat sinks.
[16] Chandra A K, Kishor K, Mishra P K and Alam M S 2015 Numerical Simulation of Heat Transfer Enhancement in Periodic Converging-diverging Microchannel *Procedia Engineering* **127** 95-101.
[17] Chai L, Xia G D and Wang H S 2016 Parametric study on thermal and hydraulic characteristics of laminar flow in microchannel heat sink with fan-shaped ribs on sidewalls – Part 1: Heat transfer *International Journal of Heat and Mass Transfer* **97** 1069-80.
[18] Duryodhan V S, Singh S G and Agrawal A 2014 Liquid flow through converging microchannels and a comparison with diverging microchannels *Journal of Micromechanics and Microengineering* **24** 125002.
[19] Abdelrazek A H, Alawi O A, Kazi S N, Yusoff N, Chowdhury Z and Sarhan A A D 2018 A new approach to evaluate the impact of thermophysical properties of nanofluids on heat transfer and pressure drop *Int Commun Heat Mass* **95** 161-70.
[20] Pak B C and Cho Y I 1998 Hydrodynamic and heat transfer study of dispersed fluids with submicron metallic oxide particles *Experimental Heat Transfer an International Journal* **11** 151-70.
[21] Xuan Y and Roetzel W 2000 Conceptions for heat transfer correlation of nanofluids *International Journal of heat and Mass transfer* **43** 3701-7.
[22] Yu W and Choi S U S 2003 The role of interfacial layers in the enhanced thermal conductivity of nanofluids: A renovated Maxwell model *Journal of Nanoparticle Research* **5** 167-71.
[23] Maiga S E B, Palm S J, Nguyen C T, Roy G and Galanis N 2005 Heat transfer enhancement by using nanofluids in forced convection flows *International journal of heat and fluid flow* **26** 530-46.
[24] Liu D and Yu L 2011 Single-phase thermal transport of nanofluids in a minichannel *Journal of Heat Transfer* **133**.
[25] Abdolbaqi M K, Mamat R, Sidik N A C, Azmi W H and Selvakumar P 2017 Experimental investigation and development of new correlations for heat transfer enhancement and friction factor of BioGlycol/water based TiO2 nanofluids in flat tubes.
[26] Xia G D, Liu R, Wang J and Du M 2016 The characteristics of convective heat transfer in microchannel heat sinks using Al2O3 and TiO2 nanofluids *Int Commun Heat Mass* **76** 256-64.